Design and Implementation of a Data Acquisition System for Rocket Motor Testing and Performance Analysis

Saptak Das* and Joseph Clary†
Georgia Institute of Technology, Atlanta, Georgia, 30332

This paper explores the design, implementation, and performance analysis of the Ramblin' Rocket Club (RRC) propulsion Data Acquisition (DAQ) system, emphasizing its role in ensuring the safety and reliability of solid rocket propulsion systems through data collected during testing. Specifically, the paper examines the hardware and software components of the RRC DAQ system and their effectiveness in capturing critical motor parameters. The system was tested during a propellant characterization campaign and a static rocket motor test, where sensors were placed on the motor to measure chamber pressure, thrust, and motor casing temperature. Data were collected at high frequencies and then transmitted and stored locally on a PC for offline analysis. This information was then visualized and processed through a specialized post-test analysis dashboard to identify trends and anomalies. The RRC DAQ system successfully collected real-time pressure, load, and temperature data with high accuracy. Through further data analysis, the DAQ system enabled the identification of thrust variations and chamber pressure inconsistencies, indicating potential performance issues that could impact motor reliability. This study underscores the critical role of a robust DAQ system for rocket motor testing by enabling real-time monitoring and detailed post-test analysis. Ultimately, the system enhances safety, performance, and reliability of rocket propulsion, reducing risks and contributing to the success of space missions.

I. Nomenclature

t_i	=	ignition delay time
t_r	=	ignition rise time
t_b	=	burning time
t_a	=	action time
F	=	thrust
m	=	propellant mass
g_0	=	gravitational acceleration
I_{total}	=	total impulse
I_{sp}	=	specific impulse
r	=	burn rate
p	=	chamber pressure
a	=	burn rate coefficient
n	=	burn rate exponent

II. Introduction

A DAQ system is designed to capture real-time data from various sensors, ensuring that a rocket motor operates within specified limits. These data are transmitted and stored for post-test analysis, allowing engineers to evaluate motor performance, assess safety margins, and detect potential anomalies before incorporating a new motor on a rocket. The purpose of this paper is to explore the design, implementation, and performance analysis of the RRC DAQ system.

*Undergraduate Student, Daniel Guggenheim School of Aerospace Engineering, Georgia Institute of Technology, 620 Cherry Street NW, Atlanta GA 30332, AIAA Student Member, 1745275

†Undergraduate Student, Daniel Guggenheim School of Aerospace Engineering, Georgia Institute of Technology, 620 Cherry Street NW, Atlanta GA 30332, AIAA Student Member, 1400629

Specifically, this system was engineered to safely and precisely monitor thrust, chamber pressure, and motor casing temperature from an experimental rocket motor while enabling a secure operating distance of at least 1,000 feet from the test article. Additionally, its design prioritizes portability, enabling deployment in remote locations. To meet these objectives, the following core requirements were established: 1) deployable anywhere, 2) safety, 3) reliability, 4) high sample rate, 5) accurate data collection, and 6) simplicity.

III. System Overview

The DAQ system uses an National Instruments (NI) CompactDAQ 9185 chassis [1] with four NI modules, NI-9481, NI-9201, NI-9210, and NI-9237, and a custom DAQ printed circuit board (PCB). The NI-9481, a 4-Channel single pole single throw electromechanical relay module, is used as a digital switch to fire up to four electronic matches or nichrome wire igniters simultaneously. The fire signals from the NI-9481 and an arming signal from an external arming box located 250 feet away from the motor under test are received by the DAQ PCB to fire igniters [2]. The NI-9201, an 8-channel C series voltage input module, is used to collect up to two pressure transducer (PT) readings via the DAQ PCB and also determine the continuity of up to four igniters using its analog-to-digital converters (ADCs) [3]. The NI-9210, a 4-channel C series temperature input module, is used to collect temperature data from up to four thermocouples [4]. Finally, the NI-9237, a bridge analog input C series strain/bridge input module, is used to collect load cell data via a 32-pin D-sub connector [5].

The NI CompactDAQ, the DAQ PCB, and various connected sensors are within 10 to 15 feet of the experimental rocket motor. To communicate with the control station 1000 feet away, a fiber optic cable is used. Both the control station and the NI CompactDAQ use Ethernet connections, so two TP-Link MC220L media converters are used to convert electrical Ethernet signals to optical signals for transmission over the fiber optic cable and then back to electrical signals at the receiving end. At the control station, a DAQ operator receives data from, and sends commands to, the NI CompactDAQ through a custom DAQ graphic user interface (GUI) running on a personal computer (PC). Using the GUI, an operator can fire igniters, check igniter continuity, read live sensor data, save test data to file, and analyze test data. The general system overview can be seen in Fig. 1.

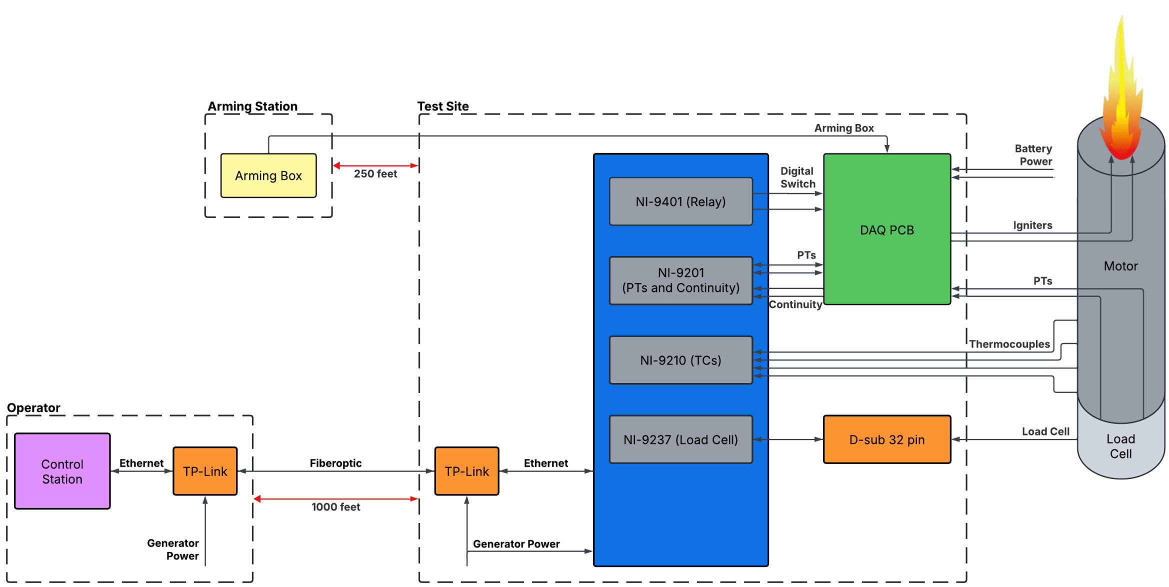

Fig. 1 DAQ System Schematic

A. DAQ Choice

The previous RRC DAQ system relied on a custom sensor configuration with an Arduino microcontroller, which struggled with reliability, data accuracy, and overall performance. As discussed further in Section III.H, these limitations prompted the transition to a commercial off-the-shelf NI CompactDAQ system to improve performance and reliability.

The NI CompactDAQ offers a modular design, enabling customization with various sensor-specific input/output modules to meet diverse data acquisition needs. Additionally, it provides high-quality sensor data at a 500 kilosample/second rate, greater flexibility in system configuration, and improved portability. Its rugged construction further ensures reliable operation in harsh environments, making it a more robust and scalable solution for long-term use.

B. Power Systems

Since the DAQ system spans 1,000 feet when deployed, relying on a single centralized power source was deemed infeasible due to significant power losses over long wire runs. Instead, a distributed power approach was determined to be more effective, utilizing separate power sources for the control station and the NI CompactDAQ. The distributed power architecture involves small, easily portable diesel generators, which supply power to the TP-Link MC220Ls and the NI CompactDAQ through their respective standard AC-to-DC converters. Additionally, the DAQ PCB is powered using two 3S lithium-polymer (LiPo) batteries, ensuring an independent and reliable power supply for its components.

A common ground must be maintained between the NI CompactDAQ and the DAQ PCB to ensure that the devices can transmit data between one another while operating on different power sources. The implementation and implications of this grounding strategy will be further discussed in Section III.E.

C. Communications

Both the NI CompactDAQ and the PC at the control station have Ethernet connections, making a direct wired connection the most straightforward approach for signal transmission. Initially, a 1000-foot Ethernet cable seemed like a viable solution. However, Ethernet signals experience significant attenuation beyond a 100-meter transmission length, leading to degradation in data quality over longer distances [6]. This limitation necessitated exploring alternative wired data transfer methods that could maintain signal integrity. After evaluating various options, a 1000-foot fiber optic cable was determined to be the most effective choice, offering minimal signal loss, higher bandwidth, and improved reliability over extended distances [7].

D. Sensors

The DAQ system interfaces with a single load cell, two pressure transducers, and four thermocouples to acquire comprehensive performance data during rocket motor tests. The LC402-10K load cell (10,000 lbf max, ±0.1% linearity, 3 mV/V output) is selected for its high load capacity and precision, ensuring that even under extreme thrust conditions measurements remain stable and repeatable. Its strain gauge-based design provides a reliable output with minimal signal noise, which is critical for accurate impulse and thrust calculations [8]. The TDH30 pressure transducers (0–5000 psi, 0–5 VDC output, 1/4" NPT Male) was chosen because the sensors' ability to handle high-pressure environments typical of a rocket motor chamber while offering a straightforward voltage output that integrates easily with the DAQ system [9]. Similarly, the use of type K thermocouples, known for their wide temperature range, durability, and cost-effectiveness, ensures that thermal data from extreme temperature regions such as the motor casing and nozzle is captured accurately [10]. Together, these sensors not only meet the stringent performance and environmental demands of rocket testing but also integrate seamlessly with the NI CompactDAQ modules, thereby ensuring reliability and simplicity in the data acquisition process.

E. DAQ PCB

The DAQ PCB is responsible for providing an interface between the NI-9201 and the PTs, firing igniters, and detecting igniter continuity. An annotated 3D rendering of the DAQ PCB is presented in Fig. 2.

To ensure reliable operation, the DAQ PCB is powered by two independent 3S LiPo batteries. One battery supplies power for logic signals across the board and the PTs, while the other is dedicated solely to igniter activation. This split power architecture was implemented to prevent sudden voltage drops across the system when igniters, drawing approximately 5 A, are fired. Without this separation, such voltage fluctuations could degrade data quality due to the power sag, potentially compromising sensor readings.

Since the DAQ PCB interfaces with the NI-9201 ADC channels while operating from a different power source, it is essential that both devices share a common ground. This common ground establishes a consistent reference point by connecting the ADC ground to the negative side of the LiPo battery powering the PTs with a wire. Without this ground reference, the voltage measured by the ADC could be incorrect since the ground of the PTs and the ground of the ADC could be at different potentials. Thus, the common ground ensures accurate sensor readings, minimizes electrical noise and signal interference, and prevents potential damage to components caused by voltage differences.

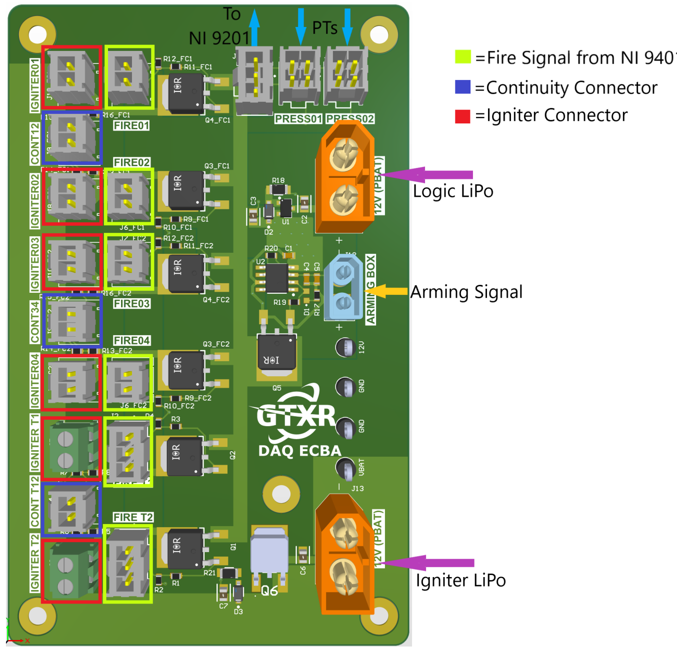

Fig. 2 Annotated 3D Rendering of the DAQ PCB

The DAQ PCB includes six independent firing channels, each equipped with corresponding connector that is fed to an ADC on the NI CompactDAQ to provide continuity readings. All electrical connections utilize Samtec Mini Mate connectors and screw terminals, chosen for their durability and quick-connect capability. To enhance safety, the firing system employs two N-type metal oxide semiconductor field effect transistors (N-MOSFETs) in series, allowing the firing channels to remain disarmed unless explicitly activated by the arming box.

The schematic of the DAQ PCB firing system is shown in Fig. 3. The igniters connect via Mini Mate connectors J8 and J10. Fire signals (Fire 1 and Fire 2) are sent from the DAQ GUI through the NI CompactDAQ, controlling the activation of N-MOSFETs Q3 and Q4, respectively. The sources of Q3 and Q4 are connected to the drain of a master arming N-MOSFET, which is only activated by a high arming signal from the external arming box. This design ensures that the low impedance firing path is only completed when both a high fire signal and a high arming signal are received, providing a robust safety interlock to prevent unintended ignition.

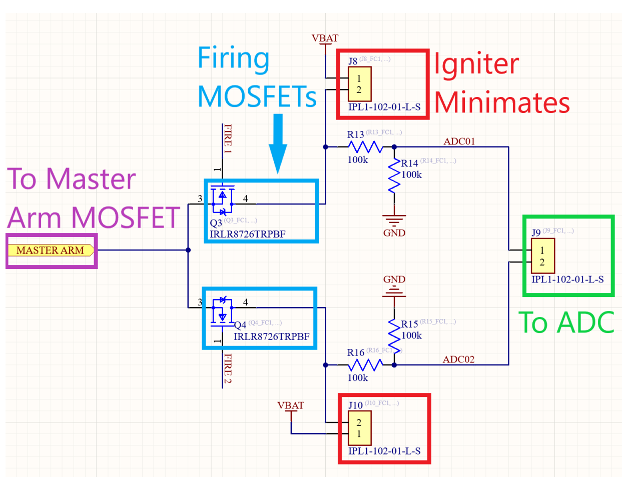

Fig. 3 Schematic of the DAQ PCB Igniter Firing System

F. DAQ GUI

The DAQ GUI was developed in Python, leveraging standard scientific computing libraries such as NumPy, SciPy, Pandas, and Matplotlib, alongside PyQt6 for the GUI itself. Prior to its implementation, the DAQ operator interacted with the hardware through a command-line interface, which posed a significant usability barrier, especially for non-technical users. Additionally, the installation process for all required software dependencies was lengthy and complex, further complicating system setup and deployment.

The introduction of the GUI-based software significantly mitigated these challenges. First, software installation was streamlined by providing standardized ZIP packages for each minor release, reducing external dependencies to just Anaconda, an open-source Python distribution platform, and NI MAX, a free software tool that allows users to access and manage National Instruments (NI) hardware and software, and automating the installation process with Windows batch and Unix bash scripts. Second, the DAQ GUI establishes a centralized dashboard that allows users to easily monitor real-time data, send fire commands, save and analyze test data, and interact with the system intuitively.

The DAQ GUI includes several key functionalities: verifying connection with the NI CompactDAQ, zeroing all sensors, issuing fire commands to two igniters simultaneously, displaying real-time sensor data both numerically and graphically, saving sensor data to files, and analyzing recorded data to compute thrust and total impulse. These enhancements have greatly improved the ease of use and simplicity of the DAQ system, making it a more robust tool for data acquisition and analysis. A picture of the DAQ GUI is presented in Fig. 4.

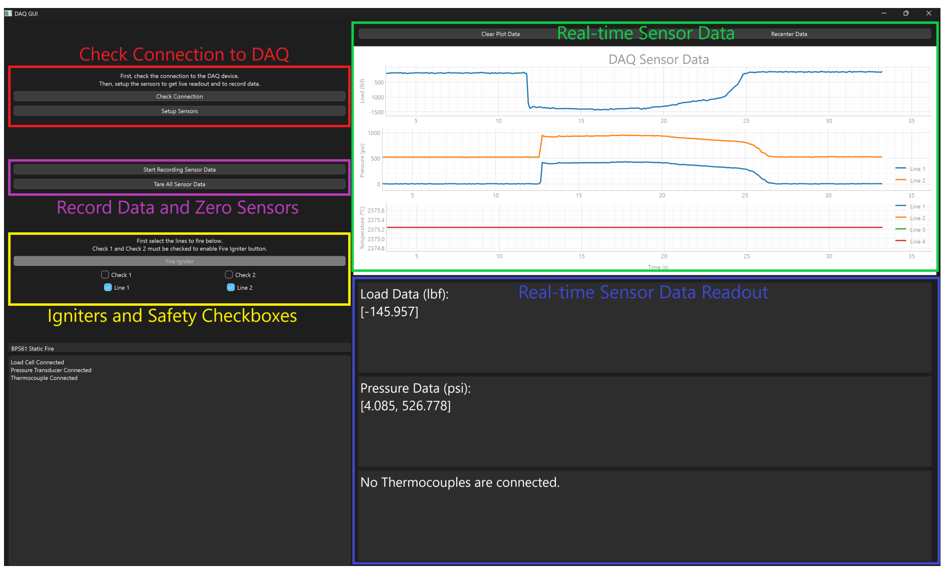

Fig. 4 Picture of the DAQ GUI interfacing with DAQ hardware

G. Data Processing and Analysis

Before the development of the DAQ GUI, all data processing and analysis was conducted manually using Matlab. Each static fire, a new Matlab script was created to analyze the data. This made the workflow unnecessarily repetitive. To streamline this process, the DAQ GUI automates data analysis, significantly reducing manual effort while improving consistency and accuracy. The implemented data processing and analysis algorithm follows the steps outlined below.

1) Raw sensor data often contains bias, which appears as a consistent offset in measurements even when no external forces or pressures are applied. This bias, caused by factors such as thermal drift, electrical offsets, or mechanical preloading, must be corrected to ensure accurate analysis. The DAQ data analysis algorithm approximates the sensor bias as the average of the pressure transducer (PT) and load cell data over a period before motor ignition. This period starts at the beginning of the data and extends until halfway through the time it takes for the sensor readings to reach 10% of the total pressure range.
2) Since sensor bias is generally a fixed offset, the pre-ignition averages are subtracted from the corresponding raw data to normalize the sensor readings.
3) A rolling median filter is applied to the data to effectively reduce noise while preserving sharp transitions, such as ignition and burnout events. Unlike low-pass or rolling average filters, which can introduce smoothing

artifacts and distort sudden changes, the median filter maintains the integrity of rapid pressure variations. While band-pass filtering is effective for isolating specific frequency components, it is less suitable for transient signals with critical time-domain features. By utilizing a median filter, the algorithm mitigates high-frequency noise and outliers while ensuring accurate detection of key events in the pressure profile.

4) After preprocessing the data, the algorithm computes key propulsion performance metrics, including maximum pressure, ignition delay time, ignition rise time, burning time, action time, total impulse, and specific impulse. This process follows the methodology outlined in Rocket Propulsion Elements by Sutton [11], which is the United States Miltary Standard used all over the world [12]. The methodology is illustrated in Fig. 5.
    1) The first step in determining the maximum pressure is to differentiate it from transient ignition spikes. This is accomplished using a histogram-based outlier filtering method. A histogram of the pressure data is generated with a sufficiently large number of bins to capture variations in pressure values. Starting from the highest recorded pressure and moving downward, bins with frequencies below a predefined threshold, indicative of short-lived ignition spikes, are removed. This process continues until a bin surpasses the frequency threshold, signifying the start of sustained combustion. By eliminating brief pressure fluctuations caused by ignition, this method ensures an accurate determination of the motor's true maximum pressure. The filtering approach is illustrated in Fig. 6a.
    2) Once the maximum pressure is determined, the ignition delay time t_i and action time t_a are extracted. The ignition delay time is defined as the duration between the start of the test and the first instance when the pressure curve reaches 10% of the maximum pressure. The action time is then computed as the interval between this first instance and the second instance when the pressure curve again crosses the 10% threshold, marking the end of the motor thrust output.
    3) The ignition rise time t_r is calculated using a similar approach. The first instance when the pressure curve reaches 75% of the maximum pressure is identified. The ignition rise time is then defined as the time interval between this moment and the first 10% threshold crossing from the previous step.
    4) To determine the end of the motor burn and derive the burning time t_b, the aft tangent bisector method is employed. This method involves drawing two tangent lines on the pressure-time curve. The first tangent is drawn along the initial descending portion of the curve, representing the onset of thrust decay. The second tangent is drawn on the opposite side of the knee, extending from the latter part of the pressure curve just before combustion fully concludes. The angle between these two tangents is then bisected, and the intersection of this bisector with the pressure-time curve defines the burn end time. The burning time t_b is calculated as the difference between this burn end time and the ignition time identified in a previous step. Although the aft tangent bisector method is widely used, it introduces a degree of subjectivity since the results depend on the chosen units for the pressure-time plot. However, this subjectivity is not a significant issue because burning time itself is an approximate value—it represents the time when the propellant web (the smallest radial thickness of propellant) is expected to be fully consumed. Due to natural non-uniformities in propellant properties, the actual location of complete burnout may vary. For mission planning, where action time is a more critical parameter, slight variations in burning time have minimal impact [13]. To ensure consistency in its implementation, the DAQ data analysis standardizes units by using MPa for pressure and seconds for time. A visual representation of the aft tangent bisector method is provided in Fig. 6b.

5) Using the action time derived above, the total impulse is computed by numerically integrating the processed load cell data over the identified period using Eq. (1).
6) Finally, specific impulse is determined from the total impulse using Eq. (2), providing a critical performance metric for evaluating the efficiency of the rocket motor.

$$I_{total} = \int_{t_i}^{t_i+t_a} F \, dt \tag{1}$$

$$I_{sp} = \frac{I_{total}}{m g_0} \tag{2}$$

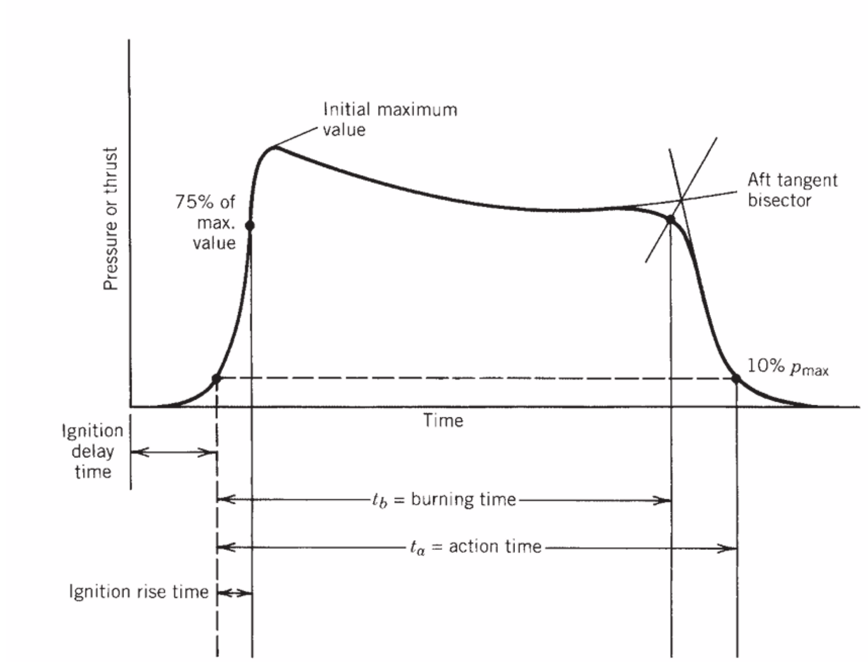

Fig. 5 Illustration of methodology outlined in Rocket Propulsion Elements [11]

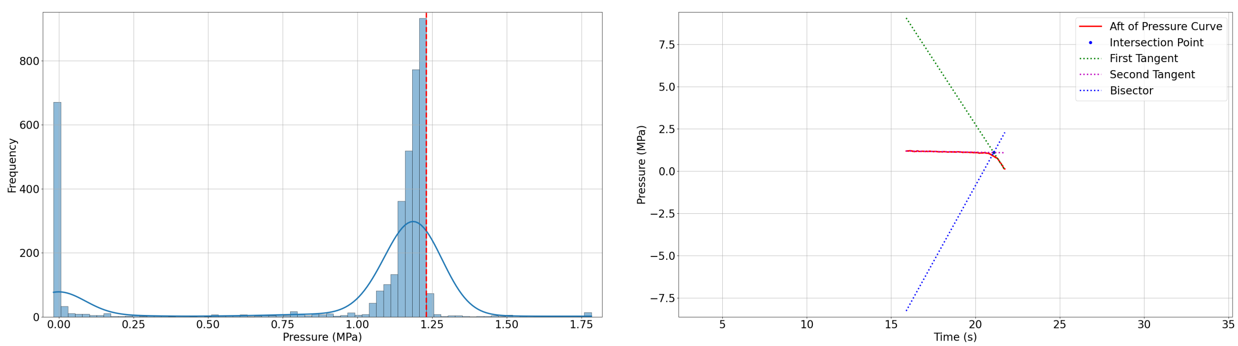

(a) Pressure Histogram for Max Pressure Detection

(b) Aft Tangent Bisector Method

Fig. 6 Implementation of methodology outlined in Rocket Propulsion Elements

H. Reliability

The reliability of the DAQ system was significantly enhanced by the transition from a custom Arduino-based setup to the modular NI CompactDAQ platform. Previously, clock drift and synchronization issues led to inconsistent data timestamps, while the limited buffer size frequently caused data loss due to overflows. Additionally, the lower resolution of the Arduino ADCs produced noisy and imprecise measurements. Finally, hardware failures resulted in intermittent operation and unexpected shutdowns, requiring frequent troubleshooting and maintenance.

In contrast, the NI CompactDAQ provides a rugged and scalable solution, featuring high-quality sensor data acquisition, customizable input/output modules, and robust construction suited for harsh environments. The NI Compact DAQ is contained within a Pelican case to further improve ruggedness and transportability. The distributed power architecture further ensures uninterrupted operation, mitigating voltage fluctuations that could otherwise degraded sensor readings. By employing a fiber optic communication link, the system also eliminates signal attenuation over long distances, maintaining data fidelity throughout testing.

Additionally, system reliability is reinforced through redundancy and fail-safe mechanisms. The DAQ PCB incorporates independent power supplies, protecting sensitive electronics from power surges caused by high-current igniter firings. The system also continuously monitors igniter continuity, enabling early detection of potential ignition failures. The combination of software-based safety checks in the DAQ GUI and hardware-level safeguards, such as the arming checkboxes and the master arming N-MOSFET for firing, further minimizes the risk of accidental ignition. These design choices collectively ensure that the DAQ system operates dependably under a variety of conditions.

I. Safety

Safety is of paramount importance when testing experimental rocket motors, particularly for the DAQ system, which is responsible for firing igniters to initiate the motor burn. Given this critical function, several key design choices were implemented throughout the DAQ system to ensure safe operation and minimize the risk of accidental ignition.

First, the DAQ firing system is always kept in a disarmed state by default, controlled via an external arming box positioned 250 feet downrange from the experimental rocket motor. Once the minimum required personnel complete their final safety checks and relocate to the control station, the system can be armed using this external box. The arming box interfaces with the DAQ PCB through an XT-30 connector. When a low arming signal is applied to the gate of the master N-MOSFET, the DAQ PCB actively prevents igniter firing, even if a fire command is sent, by significantly reducing current flow. This redundancy ensures that ignition can only occur when all safety conditions are met.

Additionally, in the event of a hang fire, the DAQ PCB is designed to monitor and detect the continuity of the igniters. This functionality is crucial for determining whether an igniter has failed to initiate combustion or if a delayed ignition is still possible. By providing real-time continuity feedback, the system enables the team to make informed decisions that prioritize safety and mitigate risks associated with misfires.

Finally, the DAQ GUI incorporates an additional safeguard by requiring two checkboxes to be manually selected before a fire command can be issued. This extra confirmation step prevents accidental ignition commands, reducing the likelihood of human error and further enhancing the overall safety, reliability, and operational security of the DAQ system.

IV. Performance Analysis using DAQ System

The RRC DAQ system successfully collected real-time pressure, thrust, and temperature data with high accuracy across multiple test campaigns, which demonstrate the system's reliability and precision. Two key examples are presented below.

A. Oxamide Propellant Characterization Campaign

GXTR recently developed a new oxamide-based solid propellant formulation. To validate its theoretical combustion characteristics, experimental data were required to determine a and n by performing a linear regression using Eq. (3). Four nozzle throat diameters were tested to evaluate the burn rate of the propellant under varying chamber pressure. The pressure data recorded during each test were processed using the DAQ GUI data analysis algorithms and are presented in Figs. 7a to 7d.

$$\ln r = \ln a + n \ln p \tag{3}$$

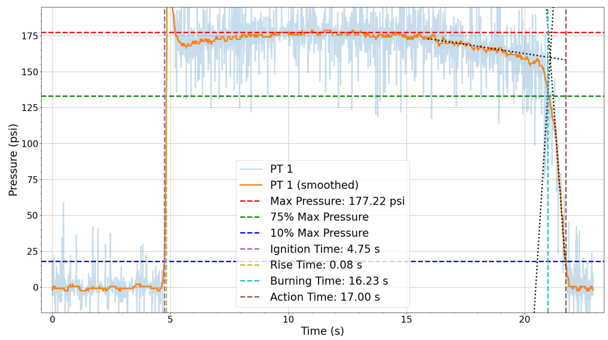

(a) 0.219 inch throat diameter

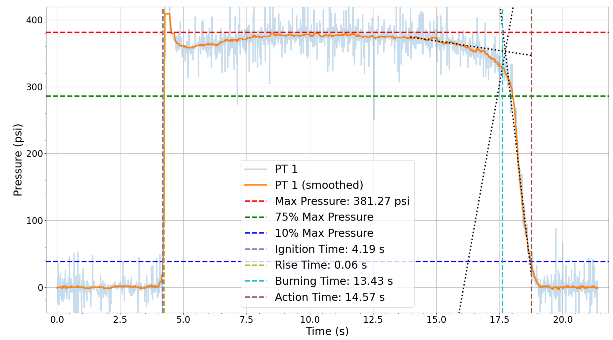

(b) 0.234 inch throat diameter

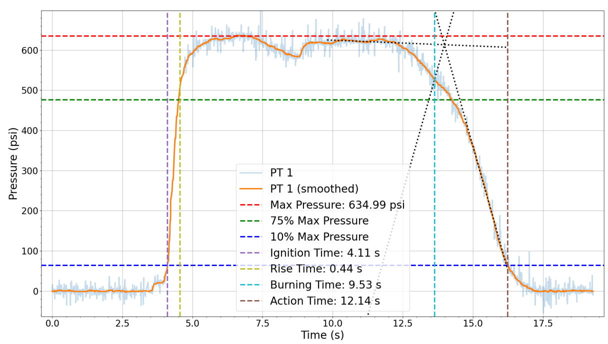

(c) 0.266 inch throat diameter

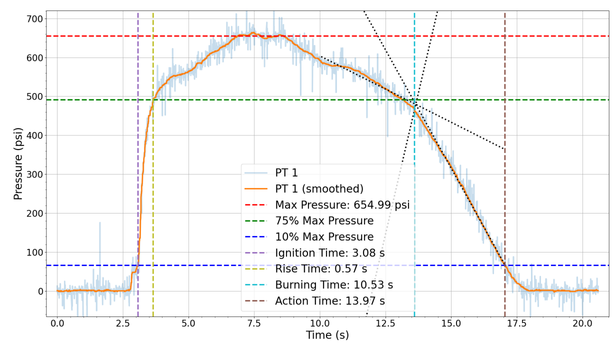

(d) 0.348 inch throat diameter

Fig. 7 Oxamide Propellant Development Pressure Data

The DAQ data analysis correctly identified the max pressure and burning time for each test. The high resolution pressure data captured by the system revealed a significant pressure spike in Figs. 7a and 7b, corresponding to the rapid combustion of residual propellant dust at ignition. This effect was absent in Figs. 7c and 7d, where different igniters with reduced propellant dust were used. Additionally, the DAQ system detected greater variability in the pressure profiles of Figs. 7c and 7d compared to the first two tests. While this inconsistency may stem from differences in igniter performance, a more probable explanation is the presence of erosive burning, which was visually confirmed during testing. By capturing transient fluctuations in chamber pressure, the DAQ system enabled a detailed analysis of erosive burning, a phenomenon where high-velocity gas flow accelerates propellant regression [14].

The advanced data acquisition capabilities of the newly developed DAQ system were critical in capturing these combustion dynamics with high precision. The system's high sampling rate and improved sensor accuracy enabled the detection of transient pressure spikes and fluctuations that would have been difficult to resolve with the previous setup. Despite variations in ignition conditions and combustion behavior, the DAQ system produced clear and comparable pressure curve profiles across all tests, demonstrating reliability in different operating conditions and reinforcing confidence in the precision and accuracy of the system. Moreover, the data analysis methods remained effective across multiple test scenarios even when anomalies were present in the data, highlighting the robustness of the algorithms used. Overall, the DAQ system provided valuable insights into the combustion behavior of the oxamide propellant, which have been used to refine the theoretical burn rate model for future motor designs.

B. BPS61 Static Fire

In December 2024, RRC conducted a static fire of BPS61, a P-class solid rocket motor developed as the booster stage for RRC's two-stage Live and Let Fly vehicle launching in summer 2025, to validate its performance against simulations.

The test setup included two PTs to measure chamber pressure and a load cell to record thrust. These measurements were processed using the automated data processing algorithms in the DAQ GUI, which removed sensor bias, filtered noise, and extracted key motor performance metrics. The recorded pressure and load cell data are presented in Figs. 8a and 8b.

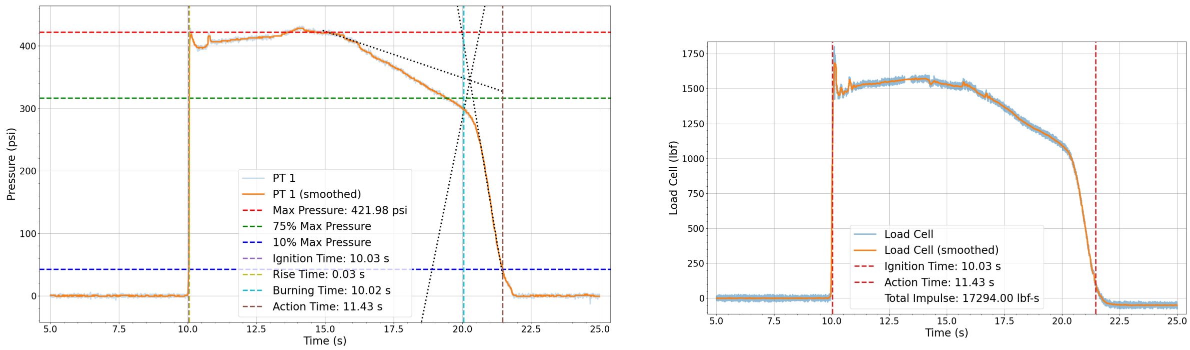

(a) BPS61 Static Fire Pressure Data

(b) BPS61 Static Fire Load Cell Data

Fig. 8 BPS61 Static Fire Data

The DAQ data analysis precisely determined that the BPS61 motor had an action time of 11.43 seconds and reached a peak pressure of 422 psi, exhibiting a slightly regressive thrust curve. The high resolution pressure and thrust data captured by the system also confirmed a total impulse of 17,294 lbf·s, classifying the motor as an upper P-class. By capturing and processing these critical parameters, the DAQ system provided a comprehensive assessment of the performance of BPS61, ensuring that no transient events or anomalies were overlooked.

These results validated that the BPS61 motor operated within expected parameters, demonstrating stable combustion and consistent thrust generation. The successful static fire test marks a significant milestone in the development of the BPS61 motor, proving its viability for integration into RRC's two-stage Live and Let Fly launch vehicle. With the accurate thrust curve derived from DAQ data, RRC can further refine and optimize the Live and Let Fly vehicle architecture before launch, following the same approach used for GTXR's Material Girl and Fire on High rockets [15] [16].

V. Conclusion

The development of the RRC DAQ system has significantly enhanced RRC's propulsion testing capabilities by providing high-fidelity, high sample rate data for performance validation. The current system design satisfies all six of the core design requirements identified in the introduction of this paper. Moreover, through rigorous experimental campaigns, including the oxamide propellant characterization and BPS61 static fire test, the DAQ system demonstrated its ability to collect accurate pressure, load, and temperature measurements with high accuracy. These data-driven insights have been instrumental in refining combustion models, validating motor performance, and informing future design iterations. Ultimately, the system enhances safety, performance, and reliability in rocket propulsion, reducing risks and contributing to the success of space missions.

Acknowledgments

The authors thank the Student Government Association at Georgia Tech and the Daniel Guggenheim School of Aerospace Engineering for logistically and financially supporting RRC. The authors thank RRC's additional financial sponsors who contribute to the success of the team. Lastly, the authors also thank the members of the RRC propulsion and avionics teams for assistance in the design and manufacture of the DAQ system and in testing operations.

References

[1] NI, "cDAQ-9185," , Jan 2024. URL `https://www.ni.com/en-us/shop/model/cdaq-9185.html`.

[2] NI, "NI-9481," , Jan 2024. URL `https://www.ni.com/docs/en-US/bundle/ni-9481-specs/resource/373507d.pdf`.

[3] NI, "NI-9201," , Jan 2024. URL `https://www.ni.com/en-us/shop/model/ni-9201.html`.

[4] NI, "NI-9210," , Jan 2024. URL https://www.ni.com/en-us/shop/model/ni-9210.html.

[5] NI, "NI-9237," , Jan 2024. URL https://www.ni.com/en-us/shop/model/ni-9237.html.

[6] Saneeha, A., "Signal Attenuation in Networking Cables: Causes, Effects, and Solutions," , Dec 2024. URL https://www.iplocation.net/signal-attenuation-in-networking-cables-causes-effects-and-solutions.

[7] Lindenphotonics, "Fiber optic cable distance: A comprehensive guide," , Nov 2024. URL https://www.lindenphotonics.com/fiber-optic-cable-distance-a-comprehensive-guide.

[8] DwyerOmega, "LC402-10K," , Sep 2024. URL https://www.dwyeromega.com/en-us/low-profile-tension-compression-load-cells-for-industrial-weighing/LC402/p/LC402-10K.

[9] Transducers-Direct, "TDH30 pressure transducer," , Feb 2025. URL https://transducersdirect.com/products/pressure-transducers/standard-pressure-transducers/tdh30-pressure-transducer/.

[10] DigiKey, "TP 29," , Feb 2025. URL https://www.digikey.com/en/products/detail/b-k-precision/TP-29/43536.

[11] Sutton, G., and Biblarz, O., *Rocket Propulsion Elements*, A Wiley Interscience publication, Wiley, 2017. URL https://www.wiley.com/en-us/Rocket+Propulsion+Elements%2C+9th+Edition-p-9781118753651.

[12] Fry, R. S., "Solid propellant subscale burning rate analysis methods for U.S. and selected NATO facilities," , Jan 2002. URL https://apps.dtic.mil/sti/tr/pdf/ADA399211.pdf.

[13] Mannepalli, R. Y., "Rao's Method and Chord-Midpoint Method for Burning Time Computation of Solid Rocket Motors," *AIAA Journal*, 2021. https://doi.org/10.2514/6.2021-3700, URL http://dx.doi.org/10.2514/6.2021-3700.

[14] King, M. K., "Erosive burning of solid propellants," *Journal of Propulsion and Power*, Vol. 9, No. 6, 1993, pp. 785–805.

[15] Garud, P., Johnson, C., and de Toledo, A. L., "Material Girl Launch Report," , 2024. https://doi.org/10.48550/ARXIV.2411.00807, URL https://arxiv.org/abs/2411.00807.

[16] Garud, P., and Lagares de Toledo, A., "Fire on High Launch Report," Tech. rep., Ramblin Rocket Club, 2024. URL rocketry.gatech.edu.